CHEMISTRY
AN ASIAN JOURNAL

DOI: 10.1002/asia.200700005

# Alkali-Metal Pyrazolate Complexes with Unusual Pyrazolate Coordination Modes and Pseudocubane Motifs

**Samar Beaini, Glen B. Deacon,* Anja P. Erven, Peter C. Junk,* and David R. Turner[a]**

**Abstract:** The dimeric complex $[Li(Ph_2pz)(OEt_2)]_2$ (**1**) and tetrameric cluster $[Na(Ph_2pz)(thf)]_4$ (**2**) were prepared by treatment of alkali-metal reagents (*n*BuLi and $Na\{N(SiMe_3)_2\}$, respectively) with 3,5-diphenylpyrazole ($Ph_2pzH$) in $Et_2O$ (**1**) or THF (**2**). The polymer $[Na(tBu_2pz)]_n$ (**3**) was obtained from reaction at elevated temperature in a sealed tube between Na metal and 3,5-di-*tert*-butylpyrazole ($tBu_2pzH$). The complex $[Na_4(tBu_2pz)_2(thf)_3(obds)]_2$ (**4**; obds = $(OSiMe_2)_2O$) was obtained as a minor product from prolonged treatment of $tBu_2pzH$ with elemental sodium in a silicone-greased flask. All four alkali-metal pyrazolato complexes were characterized by IR and $^1H$ NMR spectroscopy and X-ray crystallography.The Li dimer **1** displays $\mu$-$\eta^2$:$\eta^1$ lithium–pyrazolato binding, in which both lithium atoms are four-coordinate. Room- and variable-temperature NMR studies ($^1H$, $^{13}C$, and $^7Li$) of **1** suggest similar behavior in solution, with peaks coalescing at low temperatures. Complexes **2** and **4** display distorted cubane structures. In **2**, all the sodium atoms are five-coordinate, whereas **4** contains two sodium/pyrazolate/thf clusters (4:2:3 ratio) bridged by two $obds^{2-}$ units, as well as two four-coordinate and two five-coordinate sodium atoms. Compound **3** is composed of two independent chains with the unusual coordination modes $\mu_3$-$\eta^5$:$\eta^2$:$\eta^2$, $\mu_3$-$\eta^5$:$\eta^2$:$\eta^1$, and $\mu_3$-$\eta^4$:$\eta^2$:$\eta^1$, with five-, six-, and seven-coordinate sodium atoms. Two oxo-centered $M_8$ cage complexes $[(tBu_2pz)_6Li_8O]$ (**5**) and $[(tBu_2pz)_6Na_8O]$ (**6**) were obtained as by-products from attempted preparation of $[Li(tBu_2pz)]$ and $[Na(tBu_2pz)]$, respectively, and their structures were determined.

**Keywords:** cubane · lithium · oxo ligands · pyrazolate · sodium

## Introduction

The chemistry of pyrazolate (pz) ligands[1] has become a popular research area, owing to the observation of increasingly versatile binding modes[2] and the enhancement of the scope of $\eta^2$ binding from f-block elements to main-group and d-block elements,[3–5] as well as their role as precursors to scorpionate ligands.[6] Although bridging coordination modes are still dominant in main-group and d-block transition-metal pyrazolate complexes, recent advances in this field have found an increasing number of $\eta^2$-coordinated complexes.[3–5,7,8] The polynuclear potassium pyrazolato species obtained by Winter and co-workers,[2j] $[K(Ph_2pz)(thf)]_6$, was the first structurally documented Group 1 complex to contain the $\eta^2$ pyrazolato coordination unit, which was incorporated into the then new $\mu_3$-$\eta^1$:$\eta^2$:$\eta^1$ arrangement. It was suggested that this type of bonding should be common among Group 1 metal derivatives, and this was further supported by the subsequent isolation of the monomeric $[K(\eta^2\text{-}3,5\text{-}Ph_2pz)(\eta^6\text{-}18\text{-crown-}6)]$.[7] Novel features of the potassium complexes include a case of $\pi$-$\eta^2$ K coordination[7] and examples of "slipped", unsymmetrical $\eta^2$ binding, thus suggesting possible reversion to $\eta^1$ binding with the smaller $Na^+$ or $Li^+$ cations. Alternatively, if bridging prevails, the $\mu$-$\eta^1$:$\eta^2$:$\eta^1$ arrangement observed with potassium may be curtailed to the rare $\mu$-$\eta^1$:$\eta^2$ mode, which has been observed only twice before.[2g,9]

As part of our study of the binding modes of pyrazolate ligands with lanthanoid and main-group elements,[2b–i,4a,5a–c] we report herein the synthesis and structural characterization of $[Li(Ph_2pz)(OEt_2)]_2$ (**1**), $[Na(Ph_2pz)(thf)]_4$ (**2**), $[Na(tBu_2pz)]$ (**3**), and $[Na_4(tBu_2pz)_2(thf)_3(obds)]_2$ (**4**). These complexes illustrate the wide variety of coordination modes possible for pyrazolate ligands, including the appearance of three new binding modes, with **2** and **4** providing variations on the cubane structural theme. Since this work was com-

[a] S. Beaini, Prof. Dr. G. B. Deacon, Dr. A. P. Erven, Prof. Dr. P. C. Junk, Dr. D. R. Turner
School of Chemistry, Monash University
P.O. Box 23, Clayton, Vic 3800 (Australia)
Fax: (+61) 3-9905-4597
E-mail: glen.deacon@sci.monash.edu.au
peter.junk@sci.monash.edu.au

  

pleted, a number of related lithium and sodium pyrazolates have been reported.[9] We also report the structures of oxo-centered $M_8$ cages $[(t\mathrm{Bu_2pz})_6\mathrm{Li_8O}]$ (**5**) and $[(t\mathrm{Bu_2pz})_6\mathrm{Na_8O}]$ (**6**), obtained as by-products.

## Results and Discussion

### Synthesis and Structure of $[\mathrm{Li(Ph_2pz)(OEt_2)}]_2$ (1)

Treatment of 3,5-diphenylpyrazole ($\mathrm{Ph_2pzH}$) with *n*BuLi at room temperature in diethyl ether ($\mathrm{Et_2O}$) afforded colorless crystals of **1** after filtration and concentration of the solution [Eq. (1)].

$$2\mathrm{Ph_2pzH} + 2n\mathrm{BuLi} \xrightarrow{\mathrm{Et_2O}} [\mathrm{Li(Ph_2pz)(OEt_2)}]_2 + 2n\mathrm{BuH} \qquad (1)$$

The $^1$H NMR spectrum of the product revealed a 1:1 ratio of pyrazolate to $\mathrm{Et_2O}$ signals and showed complete conversion of the pyrazole through the absence of the NH resonance at about 10 ppm and the lack of an NH stretching absorption at 3500–3150 $\mathrm{cm^{-1}}$ in the IR spectrum. The microanalytical data suggested some decomposition of the compound during travel for analysis, despite being sealed under nitrogen.

X-ray crystallography confirmed the formation of an $\mathrm{Et_2O}$-solvated dimeric lithium pyrazolate complex (Figure 1 a), with two four-coordinate lithium ions bridged by two pyrazolate ligands bound in an $\eta^2$ fashion to one lithium ion and $\eta^1$ to the other. Thus, **1** has the highly unusual (pyrazolate) coordination of $\mu$-$\eta^2$:$\eta^1$,[2g,9] which is reminiscent of carboxylate[10] and formamidinate[11] chemistry.

The coordination sphere of the lithium ion is completed by one $\mathrm{Et_2O}$ molecule (Figure 1 a). Truncation of the $\mu_3$-$\eta^1$:$\eta^2$:$\eta^1$ coordination of $\mathrm{Ph_2pz}$ in $[\mathrm{K(Ph_2pz)(thf)}]_6$[2j] to $\mu$-$\eta^2$:$\eta^1$ in **1** can be attributed to the small size of $\mathrm{Li^+}$.[12] Similarly, the transition from $\mu$-$\eta^2$:$\eta^2$ $\mathrm{Ph_2pz}$ bridging to $\mu$-$\eta^2$:$\eta^1$ in dimeric rare-earth $[\mathrm{Ln_2(Ph_2pz)_6}]$ complexes occurs only with the smallest rare-earth metal, Sc.[2g] There is also truncation from the $\mu_3$-$\eta^1$:$\eta^1$:$\eta^1$ coordination of the pyrazolate ligand in $[\mathrm{Li}(t\mathrm{Bu_2pz})]_4$[9] owing to solvation by $\mathrm{Et_2O}$ in **1**. Recently, the structure of $[\mathrm{Li}(t\mathrm{Bu_2pz})(t\mathrm{Bu_2pzH})]_2$ has been reported as having $\mu$-$\eta^2$:$\eta^1$ binding,[9] but it displays significant differences in overall geometry from that of **1**. Whilst both complexes are nonplanar, the pyrazolato ligands in $[\mathrm{Li}(t\mathrm{Bu_2pz})(t\mathrm{Bu_2pzH})]$ are twisted further away from the Li–Li vector than in **1** (Li–N–N–Li torsion angles of 69.3 and 60.2°, respectively) to accommodate the greater steric bulk of the *t*Bu groups relative to the phenyl groups. Furthermore, the former complex has a strong hydrogen-bonding contact from the pyrazole NH group to the center of the pyrazolate ring (H···cen = 2.40 Å);[9] there is no equivalent contact in **1**. The twisting of the ligand in turn brings about a shorter Li(1)–Li(1)* distance in $[\mathrm{Li}(t\mathrm{Bu_2pz})(t\mathrm{Bu_2pzH})]_2$ compared to **1** (2.587 and 2.829 Å, respectively). As a further consequence, the difference between the Li–N bond length in the $\eta^1$ interaction and the corresponding nonbonding Li···N distance is greater in **1** (0.90 Å) than in $[\mathrm{Li}(t\mathrm{Bu_2pz})(t\mathrm{Bu_2pzH})]_2$ (0.751 Å), thus making the attribution of $\mu$-$\eta^2$:$\eta^1$ bonding in the present case clearer. In $[\mathrm{Sc_2(Ph_2pz)_6}]$,[2] the difference between bonding and nonbonding Sc–N distances in the $\mu$-$\eta^2$:$\eta^1$ interactions is 0.76–0.82 Å, whereas the largest difference between M–N bond lengths in cases of proposed $\eta^2$ binding (slipped $\eta^2$) of triazolates and pyrazolates is about 0.60 Å.[2h,13] The less-twisted orientation of the pyrazolato ligands in **1** gives rise to greater variation in the Li–N bond lengths in the $\eta^2$ interaction (difference = 0.25 Å) than in $[\mathrm{Li}(t\mathrm{Bu_2pz})(t\mathrm{Bu_2pzH})]$ (difference = 0.10 Å) (Table 1). This asymmetric bonding is also reflected by the larger N(2)–N(1)–Li(1) angle (82.25(11)°) with respect to N(1)–N(2)–Li(1) (60.01(9)°; Table 1). Comparable variations in Li–N

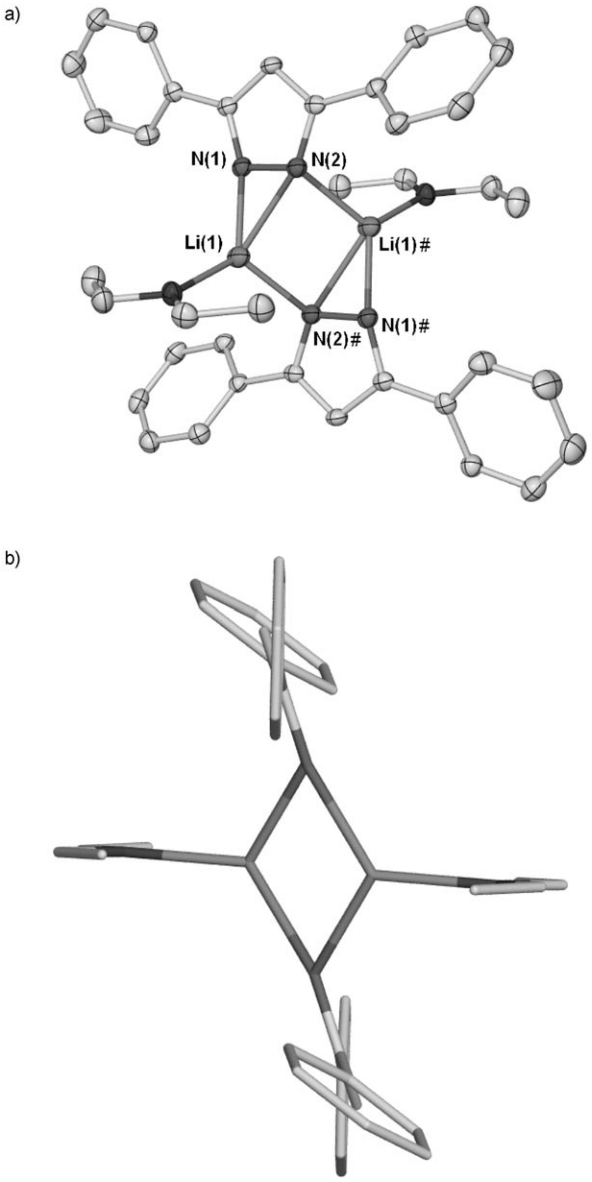


Figure 1. X-ray crystal structure of the dimeric $[\mathrm{Li(Ph_2pz)(OEt_2)}]_2$ (**1**) showing a) the atom labels and b) the relative orientations of the phenyl rings. Symmetry operator: # = 1−*x*, 2−*y*, −*z*. Ellipsoids are shown at 50% probability. Selected bond lengths and angles are listed in Table 1.

  

Table 1. A comparison of selected bond lengths (Å) and angles (°) for **1**, $[Li(Ph_2pz)(Ph_2pzH)]_2$, **2**, and $[Na(Me_2pz)(thf)]_4$.[a]

| $[Li(Ph_2pz)(OEt_2)]_2$ (**1**) | | $[Li(tBu_2pz)(tBu_2pzH)]_2$[9] | | $[Na(Ph_2pz)(thf)]_4$ (**2**) | | $[Na(Me_2pz)(thf)]_4$[9] | |
|---|---|---|---|---|---|---|---|
| Li(1)−O(1) | 1.945(3) | | | Na(1)−O(1) | 2.270(2) | Na(2)−O(1) | 2.330(1) |
| Li(1)−N(1) | 1.954(3) | Li(1)−N(1) | 2.009(4) | Na(1)−N(1) | 2.866(3) | Na(2)−N(3) | 2.757(2) |
| Li(1)−N(2) | 2.235(3) | Li(1)−N(2) | 2.022(4) | Na(1)−N(2) | 2.426(3) | Na(2)−N(4) | 2.448(2) |
| Li(1)−N(2)# | 2.042(3) | Li(1)−N(2 A) | 2.048(4) | Na(1)−N(1)† | 2.345(2) | Na(2)−N(1) | 2.382(2) |
| | | | | Na(1)−N(3)† | 2.438(3) | Na(2)−N(4)* | 2.401(2) |
| N(1)−Li(1)−N(2) | 37.71(7) | N(1)−Li(1)−N(2) | 39.73(10) | N(1)−Na(1)−N(2) | 28.68(7) | N(1)−Na(1)−N(2) | 30.88(5) |
| N(2)-N(1)-Li(1) | 82.25(11) | | | | | | |
| N(1)−N(2)−Li(1) | 60.01(9) | | | | | | |

[a] Symmetry operators: #=1−$x$, 2−$y$, −$z$; †=−$x$, $y$, −$z$+½; *=$x$, $y$, −$z$+½.

distances, similar bond-length values, and similar bond-angle variations were observed in the dimer $[Li(\mu\text{-}\eta^2{:}\eta^1\text{-TolForm})(OEt_2)]_2$[14] (TolForm = *N,N′*-di(*p*-tolylformamidinate)). A further example of the $\eta^2{:}\eta^1$ binding mode in a bidentate N-donor ligand was observed in a ruthenium triazenide complex.[15] The Li–$OEt_2$ interaction is within the normal range for Li–O distances for dimeric structures and is comparable with that in both $[Li(TolForm)(OEt_2)]_2$[14] and $[Li\{N(SiMe_3)_2\}(OEt_2)]_2$.[16] Another interesting feature of the structure of **1** is that the phenyl rings are in different positions with respect to the plane of the pyrazolate (Figure 1b). Planar angle calculations showed that one phenyl ring is close to being coplanar with the pyrazolate ring (19.43(8)°), whereas the other adopts a more-intersecting orientation (37.97(5)°).

The $^7$Li NMR spectra of **1** at room temperature in both $C_6D_6$ and $C_7D_8$ showed four different lithium resonances (two major and two minor signals) that are consistent with the $^1$H and $^{13}$C NMR spectra, both of which showed overlapping signals corresponding to $Ph_2pz^-$ and $Et_2O$ at room temperature. Notably, there are two *ortho*- and two *meta*-carbon resonances. Plausibly, a series of exchange equilibria are set up at room temperature between the fully solvated lithium complex $[Li(Ph_2pz)(OEt_2)]_2$, the partly desolvated dimer, and the unsolvated dimer and/or trimer, and so on [Eq. (2)].

$$n\,[Li(Ph_2pz)(OEt_2)]_2 \rightleftharpoons n\,OEt_2 + n\,[Li_2(Ph_2pz)_2(OEt_2)] \rightleftharpoons 2n\,OEt_2 + n\,[Li_2(Ph_2pz)_2] \rightleftharpoons [Li(Ph_2pz)]_{2n} \quad (2)$$

Variable-temperature $^1$H NMR spectra of **1** in $C_7D_8$ showed that the multiple signals observed for both $Ph_2pz^-$ and $Et_2O$ coalesced at 30 °C, as the temperature is decreased. At −40 °C one major species, plausibly $[Li(Ph_2pz)(OEt_2)]_2$, is clearly dominant, with the three minor $Et_2O$ resonances seen at 30 °C much less evident at −40 °C. A similar temperature-dependent phenomenon was observed for the lithium dimer $[\{Li(N(SiMe_3)CH_2CH_2N(SiMe_3))Li(OEt_2)\}_2]$; the compound was found to undergo rapid exchange between complexed and uncomplexed diethyl ether adducts.[17]

The $^7$Li NMR spectra, recorded whilst the sample was cooled in 10 °C steps from 30 to −40 °C, displayed a coalescence of the four signals seen at room temperature into a dominant single resonance (Figure 2). This behavior suggests that the main signal corresponds to the symmetrical dimeric ether-complexed solid-state structure, which should

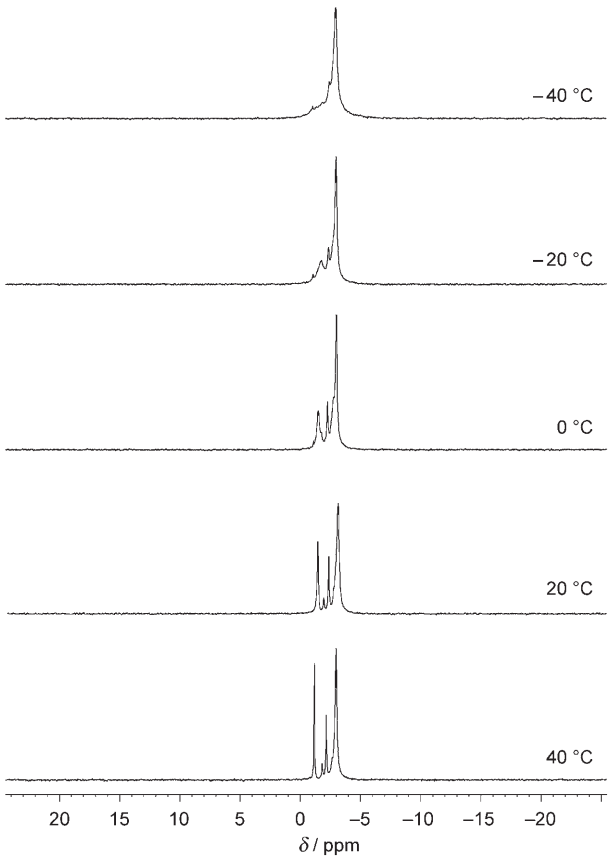


Figure 2. Selected variable-temperature $^7$Li NMR spectra of **1** in $C_7D_8$.

display only one $^7$Li resonance. An analogous shift was observed for $[8\text{-}Me_2NC_{10}H_6Li(OEt_2)]_2$ upon cooling from 0 to −90 °C, with the ether-free species $[8\text{-}Me_2NC_{10}H_6Li]_2$ observed at the highest temperature, and the etherate alone at a lower frequency at the lowest temperature.[18] A similar low-frequency shift was observed for $[Li(Me_2pz)(thf)]$ ($Me_2pz$ = 3,5-dimethylpyrazolate) on complexation of thf relative to $[Li(tBu_2pz)]_4$,[9] as well as with $[Li(thf)_nAl(Mes)_2(NH(tBu))_2]$.[19]

### Synthesis and Structure of $[Na(Ph_2pz)(thf)]_4$ (2)

$[Na(Ph_2pz)(thf)]_4$ (**2**) was prepared by treating $Na\{N(SiMe_3)_2\}$ with $Ph_2pzH$ at room temperature [Eq. (3)]. Large

  

colorless crystals were obtained after the solution was concentrated and cooled.

$$4Ph_2pzH + 4Na\{N(SiMe_3)_2\} \xrightarrow{thf} [Na(Ph_2pz)(thf)]_4 + 4HN(SiMe_3)_2 \quad (3)$$

Complete reaction was confirmed by the IR spectrum of the crystalline product, which was devoid of the NH absorption at 3400–3150 $cm^{-1}$. This was supported by the $^1H$ NMR spectrum in $C_6D_6$, which had no broad NH signal for $Ph_2pzH$ at 10 ppm and showed a $Ph_2pz$/thf ratio of 1:1. The resonances for the pyrazolate phenyl protons showed evidence of splitting, a phenomenon also observed for the thf peaks. The splitting of the signal is consistent with partial loss of thf from associated solvated sodium pyrazolate in solution [Eq. (4)].

$$[Na(Ph_2pz)(thf)]_n \rightleftharpoons m\,thf + [Na_n(Ph_2pz)_n(thf)_{n-m}] \quad (4)$$

The aggregated nature of the product was confirmed by X-ray crystallography, which revealed a tetranuclear pyrazolatosodium cage $[Na(Ph_2pz)(thf)]_4$ (**2**) (Figure 3a) comprising four sodium atoms, four tetrahydrofuran molecules, and four 3,5-diphenylpyrazolato ligands. The asymmetric unit contains half of the complex, the other half being generated by a two-fold rotation axis. Each sodium atom is five-coordinate, with $\eta^2$ coordination of one pyrazolate and $\eta^1$ binding of two adjacent pyrazolate ligands, in addition to interaction with one tetrahydrofuran molecule. The arrangement of the sodium ions and the pyrazolato ligands is analogous to the cubane-type $Na_4O_4$ cluster that is often observed, for example, in the structure of $[Na(4\text{-}MeC_6H_4O)(dme)]_4$[20] (dme = 1,2-dimethoxyethane) and is also seen with lithium[21] and potassium phenolates.[22] Recently, the cubane motif was seen in an extended form in an $Na_9O_9$ cluster that forms four face-sharing cubes.[23] Complex **2** represents, to the best of our knowledge, the closest example to a cubane geometry in which $\mu_3$-bridging pyrazolato ligands replace $\mu_3$ oxygen atoms; the only other $Na_4pz_4$ cluster, $[Na(Me_2pz)(thf)]_4$, is more significantly distorted.[9] We previously published an unsolvated $Tl_4pz_4$ cluster, $[Tl(Ph_2pz)]_4$,[2i] with a similar metal-ion arrangement, although two of the pyrazolato ligands bridge with the $\mu_3$-$\eta^1$:$\eta^1$:$\eta^1$ rather than the $\mu_3$-$\eta^1$:$\eta^2$:$\eta^1$ arrangement observed in **2** and $[Na(Me_2pz)(thf)]_4$, presumably due to the larger ionic radius of thallium.[24] The $\mu_3$-$\eta^1$:$\eta^2$:$\eta^1$ coordination mode was first observed in the analogous $[K(Ph_2pz)(thf)]_6$, in which a larger cage than a cube was obtained.[2j] The cubic motif within **2** is best seen when the midpoints of the pyrazolate N–N bonds are used to form the vertices of the cube (Figure 3b). The replacement of oxygen bridges results in a significant distortion of the cube with corner angles in the range 81.05–100.00°. The same angles within $[Na(Me_2pz)(thf)]_4$ are in the range 73.86–106.03°, which confirms a greater distortion than in **2**.

The $\eta^2$ binding of the 3,5-diphenylpyrazolate ligands to the sodium atoms comprises Na(1)–N(1)/N(2) and Na(2)–N(3)/N(4) interactions, whereas the $\eta^1$ interactions are through N(1)–Na(1)†, N(2)–Na(2), N(3)–Na(1)†, and N(4)–Na(2)† contacts. Whereas most Na–N bond lengths are near 2.40 Å, Na(1)–N(1) and Na(2)–N(4) distances are considerably longer, as part of a skewed $\eta^2$ binding. The range of Na–N distances is similar to but slightly larger (≈0.1 Å) than that observed for $[Na(Me_2pz)(thf)]_4$, and the bite angles are

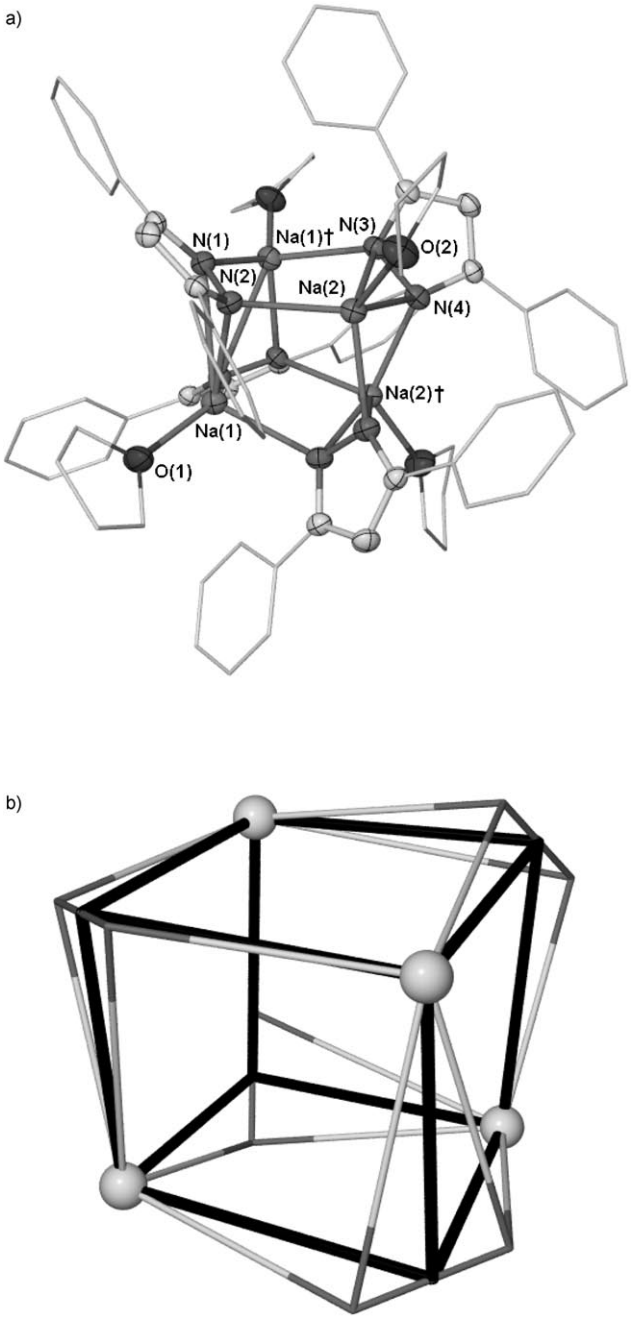


Figure 3. a) X-ray crystal structure of the tetranuclear sodium cluster $[Na(Ph_2pz)(thf)]_4$ (**2**) showing the atom labels (ellipsoids shown at 50% probability). b) The cubane-type geometry adopted by the $Na_4pz_4$ unit (sodium atoms shown as spheres); heavy lines are formed between Na and the N–N centroids. Selected bond lengths and angles are reported in Table 1. Symmetry operator: † = $-x$, $y$, $\frac{1}{2}-z$.

  

CHEMISTRY
AN ASIAN JOURNAL

smaller for **2** than for the $Me_2pz$ complex.[9] Both effects reflect the greater bulk of $Ph_2pz$ relative to $Me_2pz$. All values are within the wider range observed for the Na–N bonds of $[Na\{Ln(t\mathrm{Bu}_2pz)_4\}]_n$ complexes.[2h]

### Synthesis and Structure of the Polymeric Unsolvated $[Na(t\mathrm{Bu}_2pz)]_n$ (3)

The double-stranded sodium 3,5-di-*tert*-butylpyrazolate polymers $\{[Na(t\mathrm{Bu}_2pz)]_3\}_\infty$ and $[Na(t\mathrm{Bu}_2pz)]_6\}_\infty$ were first obtained as by-products in the high-temperature reaction between Yb metal filings, Na metal, and $t\mathrm{Bu}_2pz\mathrm{H}$. They were then deliberately prepared in a sealed Carius tube by direct treatment of $t\mathrm{Bu}_2pz\mathrm{H}$ with Na metal at 200 °C [Eq. (5)].

$$n\mathrm{Na} + nt\mathrm{Bu}_2pz\mathrm{H} \xrightarrow{200^\circ\mathrm{C}} [\mathrm{Na}(t\mathrm{Bu}_2pz)]_n + \frac{n}{2}\mathrm{H}_2 \qquad (5)$$

Use of a 50% excess of sodium metal ensured full consumption of the $t\mathrm{Bu}_2pz\mathrm{H}$ ligand. This complex was obtained earlier by reaction of sodium metal with pyrazole in THF, but attempts to obtain crystals gave the cage $[Na_7(OH)(t\mathrm{Bu}_2pz)_6]$.[9] The $^1$H NMR and IR spectra of **3** showed the presence of the pyrazolate ligand and neither an NH resonance nor a $\nu$(NH) absorption. X-ray crystal-structure determination showed two independent sodium pyrazolate polymer strands, in which nine unique sodium atoms (six in one strand, three in the other) are surrounded by only pyrazolate ligands (nine independent) (Figure 4).

The structure differs from the single ladder recently observed in $[K(t\mathrm{Bu}_2pz)]_n$, which has only one unique potassium atom.[9] More significantly, the present complex exhibits the new pyrazolate binding modes $\mu_3$-$\eta^5$:$\eta^2$:$\eta^2$, $\mu_3$-$\eta^5$:$\eta^2$:$\eta^1$, and $\mu_3$-$\eta^4$:$\eta^2$:$\eta^1$ (6:2:1), in contrast with the (new) $\mu_3$-$\eta^5$:$\eta^4$:$\eta^2$ ligation of the potassium derivative.[9] Each sodium atom is bound by three bridging ligands either through an $\eta^5$ and two $\eta^2$ interactions (formal seven-coordination), an $\eta^5$, an $\eta^2$, and an $\eta^1$ interaction (formal six-coordination), or $\eta^4$, $\eta^2$, and $\eta^1$ interactions (formal five-coordination). In the chain with six unique sodium atoms, two pairs of seven-coordinate sodium atoms (Na(1,2) and Na(5,6)) flank two six-coordinate ones (Na(3,4)). By contrast, the three-sodium chain has two seven-coordinate sodium atoms (Na(9,8)) followed by a five-coordinate sodium atom (Na(7)).

In the three cases in which $\eta^1$ (N) rather than $\eta^2$ ($N_2$) ligation is proposed, the difference between $Na–N_{bonding}$ and $Na\cdots N_{nonbonding}$ is 0.8–0.9 Å (Table 2), which is comparable to the analogous differences in **1** and $[Sc_2(Ph_2pz)_6]$.[2g] Furthermore, the corresponding $Na–N_{bonding}–N_{nonbonding}$ and $Na–N_{bonding}–C_{nonbonding}$ angles are near trigonal ($\approx$115 and 132°, respectively). Virtually all the $\eta^2$ bonding interactions (components of more-complex binding modes) are highly unsymmetrical (slipped),[2j] with differences between the two Na–N bond lengths in the range 0.09–0.62 Å (Table 2). Values near the upper limit have been reported for slipped $\eta^2$ binding in triazolatopotassium and $[Na\{Ln(t\mathrm{Bu}_2pz)_4\}]$ complexes.[2h,13a] Although this stretches the concept of $\eta^2$ binding to the limit, the longest proposed Na–N bonds are still 0.20 Å shorter than the Na···N distances that are considered nonbonding (Table 2) as part of the assignment of $\eta^1$ binding. Na–N bond lengths comparable to the longest Na–N values

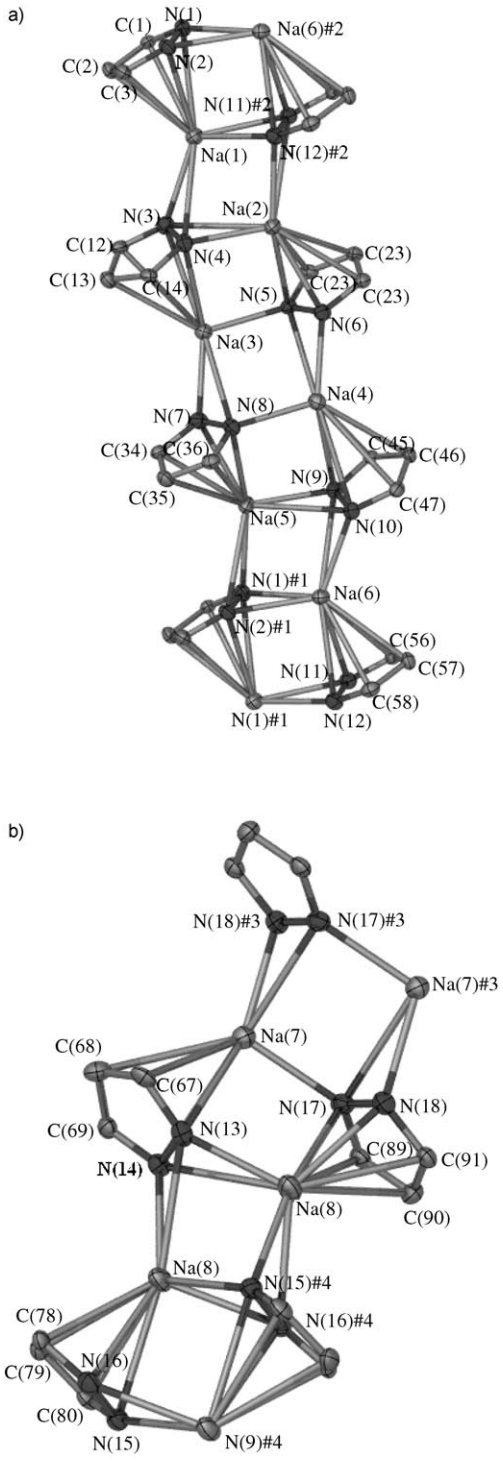


Figure 4. Structure of $[Na(t\mathrm{Bu}_2pz)]$ showing the two independent sodium pyrazolate strands a) $\{[Na(t\mathrm{Bu}_2pz)]_3\}_\infty$ and b) $\{[Na(t\mathrm{Bu}_2pz)]_6\}_\infty$. *t*Bu groups are removed for clarity, ellipsoids shown at 50% probability. Symmetry operators: #1 = $x-1$, $y$, $z$, #2 = $x+1$, $y$, $z$, #3 = $-x+1$, $-y+2$, $-z$, #4 = $-x+2$, $-y+2$, $-z$.

  

Table 2. Selected bond lengths (Å) and angles (°) for **3**.[a]

| | $\{[Na(tBu_2pz)]_6\}_n$ | | | $\{[Na(tBu_2pz)]_3\}_n$ | |
|---|---|---|---|---|---|
| Na(1)–N(1) | 2.877(4) | Na(4)–N(9) | 2.772(4) | Na(7)–N(13) | 2.717(4) |
| Na(1)–N(2) | 2.791(4) | Na(4)–N(10) | 3.023(4) | Na(7)–N(14) | 3.038(4) |
| Na(1)–C(1) | 2.896(4) | Na(4)–C(45) | 2.749(4) | Na(7)–C(67) | 2.725(4) |
| Na(1)–C(2) | 2.833(5) | Na(4)–C(46) | 2.945(5) | Na(7)–C(68) | 3.026(5) |
| Na(1)–C(3) | 2.763(5) | Na(4)–C(47) | 3.125(4) | Na(7)–C(69)* | 3.216(4) |
| Na(1)–N(3) | 2.487(4) | Na(4)–N(5) | 2.898(4) | Na(7)–N(17) | 2.348(4) |
| Na(1)–N(4) | 2.970(4) | Na(4)–N(6) | 2.368(3) | Na(7)–N(18)* | 3.210(4) |
| Na(1)–N(11)#1 | 2.527(4) | Na(4)–N(7)* | 3.216 | Na(7)–N(17)#3 | 2.906(4) |
| Na(1)–N(12)#1 | 2.412(4) | Na(4)–N(8) | 2.372(4) | Na(7)–N(18)#3 | 2.368(4) |
| | | | | | |
| Na(2)–N(5) | 2.618(4) | Na(5)–N(7) | 2.598(4) | Na(8)–N(17) | 2.624(4) |
| Na(2)–N(6) | 2.646(4) | Na(5)–N(8) | 2.636(4) | Na(8)–N(18) | 2.571(4) |
| Na(2)–C(23) | 2.789(4) | Na(5)–C(34) | 2.785(5) | Na(8)–C(89) | 2.932(4) |
| Na(2)–C(24) | 2.915(5) | Na(5)–C(35) | 2.938(5) | Na(8)–C(90) | 3.043(5) |
| Na(2)–C(25) | 2.832(5) | Na(5)–C(36) | 2.844(4) | Na(8)–C(91) | 2.838(4) |
| Na(2)–N(3) | 2.987(4) | Na(5)–N(9) | 2.359(4) | Na(8)–N(13) | 2.375(4) |
| Na(2)–N(4) | 2.369(4) | Na(5)–N(10) | 2.940(4) | Na(8)–N(14) | 2.892(4) |
| Na(2)–N(11)#1 | 3.043(3) | Na(5)–N(1)#2 | 2.413(4) | Na(8)–N(16)#4 | 2.701(4) |
| Na(2)–N(12)#1 | 2.432(4) | Na(5)–N(2)#2 | 2.944(3) | Na(8)–N(15)#4 | 2.457(4) |
| | | | | | |
| Na(3)–N(3) | 2.978(4) | Na(6)–N(11) | 2.707(4) | Na(9)–N(15) | 2.901(3) |
| Na(3)–N(4) | 2.722(4) | Na(6)–N(12) | 2.785(4) | Na(9)–N(16) | 2.851(3) |
| Na(3)–C(12) | 3.129(5) | Na(6)–C(56) | 2.747(5) | Na(9)–C(78) | 2.775(4) |
| Na(3)–C(13) | 2.999(5) | Na(6)–C(57) | 2.854(5) | Na(9)–C(79) | 2.772(5) |
| Na(3)–C(14) | 2.754(4) | Na(6)–C(58) | 2.864(4) | Na(9)–C(80) | 2.859(4) |
| Na(3)–N(5) | 2.367(4) | Na(6)–N(9) | 2.955(3) | Na(9)–N(13) | 2.915(4) |
| Na(3)–N(6)* | 3.230(4) | Na(6)–N(10) | 2.443(4) | Na(9)–N(14) | 2.446(3) |
| Na(3)–N(7) | 2.358(4) | Na(6)–N(1)#2 | 2.405(4) | Na(9)–N(15)#4 | 2.382(4) |
| Na(3)–N(8) | 2.891(4) | Na(6)–N(2)#2 | 2.498(4) | Na(9)–N(16)#4 | 2.555(4) |
| | | | | | |
| Na(1)–cen(1) | 2.579 | Na(4)–cen(4) | 2.682 | Na(7)–cen(7) | 2.649 |
| Na(2)–cen(2) | 2.500 | Na(5)–cen(5) | 2.504 | Na(8)–cen(8) | 2.549 |
| Na(3)–cen(3) | 2.673 | Na(6)–cen(6) | 2.535 | Na(9)–cen(9) | 2.577 |
| | | | | | |
| N(12)#1–Na(1)–N(11)#1 | 32.79(11) | N(6)–Na(4)–N(5) | 28.57(10) | N(18)#3–Na(7)–N(17)#3 | 28.53(10) |
| N(3)–Na(1)–N(4) | 28.02(10) | N(9)–Na(5)–N(10) | 27.93(10) | N(15)#4–Na(8)–N(16)#4 | 31.25(10) |
| N(4)–Na(2)–N(3) | 27.36(10) | N(1)#2–Na(5)–N(2)#2 | 28.07(10) | N(13)–Na(8)–N(14) | 28.56(11) |
| N(12)#1–Na(2)–N(11)#1 | 26.75(10) | N(1)#2–Na(6)–N(2)#2 | 33.05(11) | N(14)–Na(9)–N(13) | 28.42(10) |
| N(7)–Na(3)–N(8) | 28.47(10) | N(10)–Na(6)–N(9) | 28.01(10) | N(15)#4–Na(9)–N(16)#4 | 32.92(11) |

[a] Symmetry operators: #1 = $x-1$, $y$, $z$; #2 = $x+1$, $y$, $z$; #3 = $-x+1$, $-y+2$, $-z$; #4 = $-x+2$, $-y+2$, $-z$; * denotes nonbonding. [b] Na–centroid distances calculated from $\eta^5$-bound pyrazolate ligands to their respective sodium atoms.

(Table 2) have been reported for $[Na\{Ln(tBu_2pz)_4\}]$ complexes.[2h] Six of the pyrazolate ligands have $\mu$-$\eta^2$:$\eta^2$ components in their binding, but as a consequence of the asymmetry in the $\eta^2$-($N_2$)–Na bonding, the intersection angle between the $NaN_2$ and pyrazolate planes varies widely from the 45° of symmetrical binding (19.14–61.23°). By contrast, the corresponding angles for the $\eta^2$ component of $\mu$-$\eta^2$:$\eta^1$ moieties have a 41.13–48.70° range. In the case of the proposed $\eta^5$ (and $\eta^4$) coordination of $tBu_2pz$, there are several ligands with a small variation (0.1–0.2 Å) between the five Na–N/Na–C bond lengths, and some with larger differences (0.3–0.4 Å) between the longest and shortest bonds (Table 2), which is indicative of a more-skewed ligation. However, the average of all five Na–N/Na–C bond lengths differs from the average Na–C bond length by less than 0.15 Å for all ligands, and usually one of the Na–C bond lengths is as short as the Na–N bond lengths. Consistent with $\pi$-$\eta^5$ (and -$\eta^4$) binding, the Na–cen–C($t$Bu) (cen = centroid of $tBu_2pz$) angles are near 90° (80.57–105.84°), with the average of two such angles per ligand closer to 90°.

The average Na–C bond lengths for the pyrazolate rings (2.802–2.961 Å), are near the reported values for cyclopentadienylsodium compounds, namely, 2.849–2.948,[24] 2.678–2.845,[25] 2.76–2.92,[26] and 2.914–2.935 Å.[27] ([Na(S)Cp] and [Na(S)$Cp^{Me}$]; Cp = cyclopentadienyl, $Cp^{Me}$ = 1,2,3,4,5-methylcyclopentadienyl, S = dme, 15[crown]-5, 18[crown]-6, or *N*,*N*,*N*′,*N*′-tetramethylethylenediamine (tmeda)).[24–27] Despite the long Na–centroid distances of Na(3), Na(4), and Na(7) from their respective $\pi$-bonded pyrazolate ligands, the average Na–$pz_{centroid}$ distances of 2.578 ($\{[Na(tBu_2pz)]_3\}_\infty$) and 2.590 Å ($[Na(tBu_2pz)]_6\}_\infty$) correspond to literature values for Na–centroid distances (e.g., 2.649[24] and 2.667 Å[27]). From consideration of bond lengths in $\pi$-arene–Na complexes, for example, [Na($\eta^6$-PhMe)Sn(Si(SiMe$_3$)$_3$)$_3$],[28] [Na($\eta^4$-PhMe)GaMe$_3$(Si(SiMe$_3$)$_3$)],[29] [Na$_6$($\eta^6$-PhMe)$_2$(SSiPh$_3$)$_6$],[30] and [Na($\eta^6$-PhMe)$_2$(Al(SiMe$_3$)$_4$)],[31]

  

CHEMISTRY
AN ASIAN JOURNAL

Na–C($t$Bu$_2$pz) distances of up to about 3.1 Å but not greater than 3.2 Å in [Na($\eta^4$-PhMe){Ln($t$Bu$_2$pz)$_4$}] were considered to be bonding.[2h] On this basis, Na(7)···C(69) (3.216(4) Å) was excluded as a bonding interaction; hence, coordination of the pyrazolate ligand N(13,14)–C(67,68,69) is viewed as $\eta^4$. Furthermore, the excluded contact is about 0.2 Å longer than the longest proposed bond from this ligand, Na(7)–N(14) (Table 2).

The $^1$H NMR spectrum of [Na($t$Bu$_2$pz)] in $C_6D_6$ at room temperature showed two pyrazolate resonances (3:1), whilst a similar spectrum in $C_7D_8$ showed one major and two minor (one broad) pz H4 resonances. At 60 °C in $C_7D_8$, these coalesced into two resonances. Upon cooling to −60 °C, the minor resonances became better-resolved (Figure 5) with a low-frequency shift and increased separation of all signals. Dissolution of the polymeric complex in $C_7D_8$ must involve truncation of the infinite chains, aided by the well-established Na–toluene coordination,[2h] resulting in a species with bridging and terminal $t$Bu$_2$pz groups. Because of the different pyrazolate coordination modes and complex bridging in the structure (Figure 4), it is likely that different terminal groups are obtained in solution. Accordingly, the main resonance is assigned to bridging $t$Bu$_2$pz ligands and the smaller peaks to terminal pyrazolate groups, with slow exchange occurring. This contrasts with the fast exchange observed for [Mg($t$Bu$_2$pz)$_2$]$_2$ in $C_6D_6$ even at low temperature.[4c]

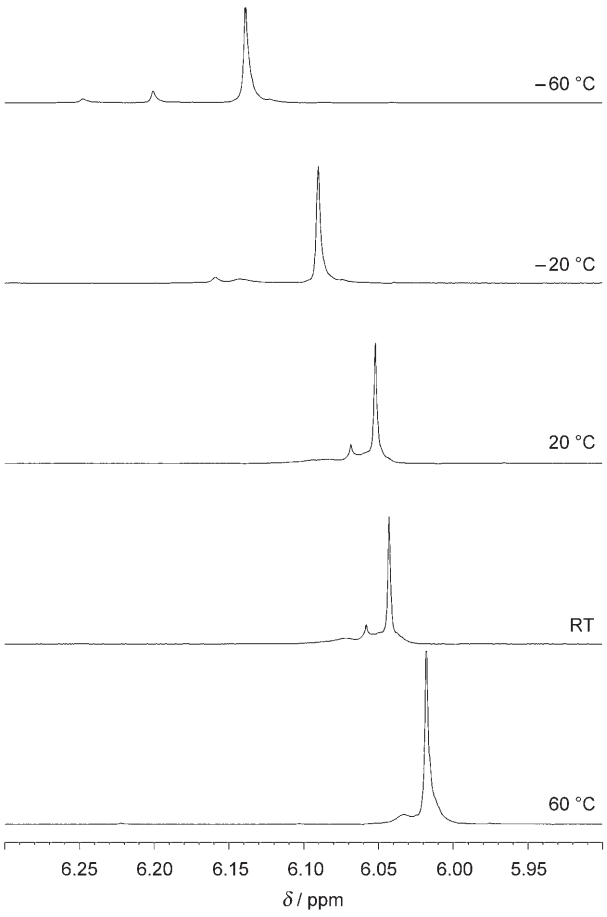


Figure 5. Variable-temperature $^1$H NMR spectra of **3** in $C_7D_8$.

### Formation and Structure of [Na$_4$($t$Bu$_2$pz)$_2$(thf)$_3$(obds)]$_2$ (4)

Upon reaction of 3,5-di-*tert*-butylpyrazole with a large excess of sodium metal in THF at room temperature over several months in a silicone-greased Schlenk flask, a small number of single crystals of the obds-bridged complex [Na$_4$($t$Bu$_2$pz)$_2$(thf)$_3$(obds)]$_2$ (**4**) was obtained [Eq. (6)].

$$(SiMe_2O)_n \xrightarrow[Na(pz)]{Na} [Na_4(tBu_2pz)_2(thf)_3(obds)]_2 \quad (6)$$

A variety of units derived from the degradation of silicone grease have been incorporated into metal–organic species[32,33] (for a review, see reference [32a]). Germane precedents for the formation of the obds anion come from the reaction of silicone grease with thallium(I) ethoxide[33a] and with barium metal and 3,5-dimethylpyrazole in tetrahydrofuran.[33b] The IR and NMR spectra of **4** showed neither a pyrazole NH absorption nor an NH resonance thereby indicating complete conversion into pyrazolate ligands. Integration of the $^1$H NMR signals gave a thf/$t$Bu$_2$pz/obds ratio of 3:2:1, and the composition of **4** was established by X-ray crystallography.

The structure of **4** consists of two tetranuclear sodium cages bridged by the obds groups. Each Na$_4$ cluster contains two $\eta^2$:$\eta^1$:$\eta^1$ pyrazolate ligands chelated to five-coordinate sodium atoms, Na(1) and Na(2). The coordination spheres of these two sodium atoms are different. Na(1) is coordinated to an $\eta^2$-pyrazolate, one thf molecule, and one oxygen atom from each obds ligand, whereas Na(2) has one of the obds oxygen atoms replaced by an $\eta^1$-pyrazolate interaction. The $\eta^2$ interactions are asymmetric with Na–N bond-length differences of 0.251 and 0.588 Å for Na(1) and Na(2), respectively (Table 3). The position of the N(3)/N(4) pyrazo-

Table 3. Selected bond lengths (Å) and angles (°) for the oxobis(dimethylsilyl oxide)-bridged complex **4**.[a]

| | | | |
|---|---|---|---|
| Na(1)–N(1) | 2.446(4) | Na(2)–N(1) | 2.442(4) |
| Na(1)–N(2) | 2.697(3) | Na(2)–N(3) | 2.446(4) |
| Na(1)–O(1) | 2.288(3) | Na(2)–N(4) | 3.034(4) |
| Na(1)–O(4) | 2.310(3) | Na(2)–O(2) | 2.337(3) |
| Na(1)–O(6)∓ | 2.256(3) | Na(2)–O(6)∓ | 2.240(3) |
| Na(3)–N(2) | 2.407(3) | Na(2)–N(2) | 3.255* |
| Na(3)–N(3) | 2.436(4) | Na(4)–N(4) | 2.392(4) |
| Na(3)–O(3) | 2.341(3) | Na(4)–O(4) | 2.271(3) |
| Na(3)–O(4) | 2.271(3) | Na(4)–O(5)∓ | 2.489(3) |
| Na(3)–N(4) | 3.116(3)* | Na(4)–O(6)∓ | 2.318(3) |
| | | Na(4)–N(3) | 3.162(3)* |
| N(1)–Na(1)–N(2) | 31.09(9) | N(3)–Na(2)–N(4) | 26.80(9) |
| N(1)–N(2)–Na(1) | 64.53(17) | N(3)–N(4)–Na(2) | 52.33(17) |
| N(2)–N(1)–Na(1) | 84.38(19) | N(4)–N(3)–Na(2) | 100.9(2) |
| N(2)–Na(3)–N(3) | 100.53(9) | | |

[a] Symmetry operator: ∓ = $-x+1$, $-y+1$, $-z$; * denotes nonbonding.

  

late means that it is close to forming an $\eta^2$ interaction with Na(4) with a nonbonding N(3)–Na(4) distance of 3.162(3) Å (compare the longest bond length (N(3)−Na(2)) of 3.03 Å). Both of these distances are well within the sum of the van der Waals radii,[34] but an upper limit of about 3.0 Å seems to be necessary for a credible Na−N bond. The more-distorted pyrazolate environment at Na(2) is also evidenced in the greater difference in the N–N–Na angles compared with those of Na(1) (Table 3). Na(3) is four-coordinate, being bound ($\eta^1$) almost symmetrically by the two pyrazolate ligands (Na(3)–N(2) = 2.407(3) Å, Na(3)–N(3) = 2.436(4) Å), one thf molecule, and one obds oxygen atom. Na(4) is near symmetrically chelated by two oxygen atoms from one obds ligand, O(5)∓ and O(6)∓, in addition to interacting with one oxygen from the other obds ligand and a pyrazolate nitrogen atom (N(4)).

The two terminal oxygen atoms of the obds ligands, O(4) and O(6), act as $\mu_3$ bridges between Na(1)/Na(3)/Na(4) and Na(1)/Na(2)/Na(4), respectively. In both cases the three Na–O interactions are similar in length, within the range 2.240–2.318 Å. These $\mu_3$-oxygen atoms act as two of the vertices of the pseudocubane geometry formed by the $Na_4$ cluster (Figure 6b), with O−Na−O angles in the range 86.74–95.73°. The two pyrazolate ligands occupy the two remaining vertices to produce a cubane-type structure that is significantly distorted at the pyrazolate end. This novel $Na_4$ cluster represents the midpoint between the traditionally observed $Na_4O_4$ clusters and the $Na_4pz_4$ pseudocube found in **2**. Similar $\mu_3$ bridging of obds to that in **4** was observed in $[Ba_6(Me_2pz)_8(thf)_6(obds)_2]$.[33b]

The bulk product could not be crystallized for X-ray crystallography and was instead analyzed by NMR and IR spectroscopy. The $^1$H NMR spectrum showed the presence of two species, one minor and one major. The main component showed a *t*$Bu_2$pz/thf ratio of 1:1, and the indicated [Na(*t*$Bu_2$pz)(thf)] species may be tetranuclear like $[Na(Ph_2pz)(thf)]_4$ (**2**). For the minor component, the *t*Bu and H4 resonances were similar to those of the main signals of [Na(*t*$Bu_2$pz)] (**3**), and no $Me_2Si$ resonance was detected. Exchange of *t*$Bu_2$pz groups between this compound and [Na(*t*$Bu_2$pz)(thf)] is evidently slow.

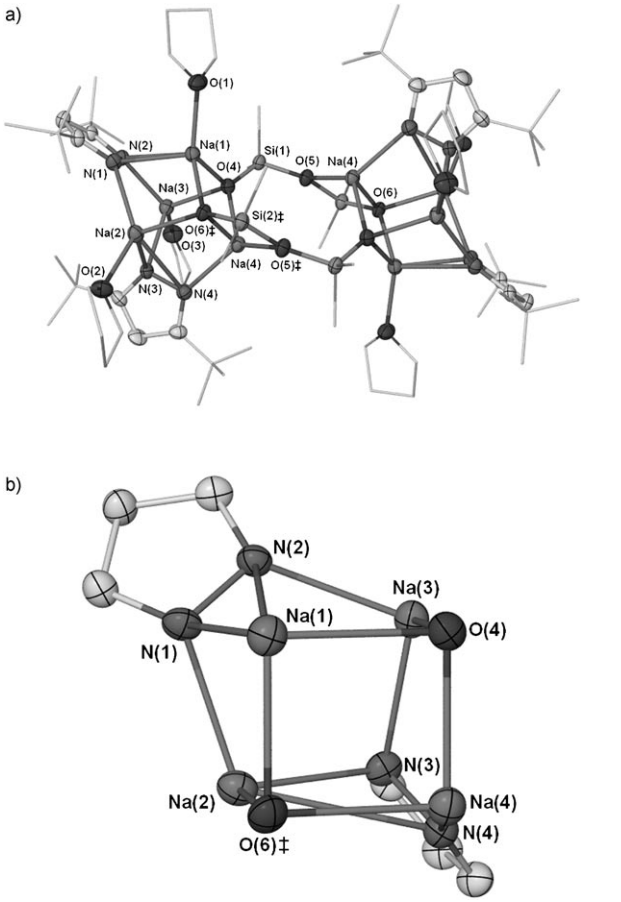


Figure 6. a) X-ray structure of the oxobis(dimethylsilyl oxide)-bridged complex $[Na_4(tBu_2pz)_2(thf)_3(obds)]_2$ (**4**). b) The pseudocubane cluster $Na_4O_2pz_2$, with *t*Bu groups, thf molecules, and obds carbon atoms omitted for clarity. Ellipsoids are shown at 50% probability. Symmetry operator: ∓ = 1−*x*, 1−*y*, −*z*.

### Structural Analysis of Li and Na Cage Complexes

The isomorphous oxygen cage complexes $[Li_8(tBu_2pz)_6O]$ (**5**) and $[Na_8(tBu_2pz)_6O]$ (**6**) (Figure 7) were produced as impurities in the attempted preparation of the respective lithium and sodium 3,5-di-*tert*-butylpyrazolates, and as such were analyzed only by X-ray crystallography and $^1$H NMR spectroscopy. The latter revealed only a single *t*Bu resonance and a single H4 resonance in each case. A contrasting asymmetric, more-open cage was observed for $[Na_7(tBu_2pz)_6(OH)]$[9] with a $\mu_7$-hydroxide core rather than the $\mu_8$-oxide of **5** and **6**.

Of the eight lithium atoms bound to the central oxygen atom in **5**, only two are unique. All lithium atoms are four-coordinate, being bound to the central oxygen atom and in an $\eta^1$ mode to the nitrogen atoms of three adjacent pyrazolate ligands. The arrangement of the lithium atoms is almost perfectly cubic, with equal Li–Li distances around the edges of the cube (2.397(11) and 2.395(12) Å). The pyrazolate ligands are situated over the center of the faces of the cube and perpendicular to it with each nitrogen atom bridging $\eta^1$:$\eta^1$ between two lithium atoms at almost-identical distances (Figure 7c, Table 4), and with the novel overall $\mu_4$-$\eta^1$:$\eta^1$:$\eta^1$:$\eta^1$ coordination first reported recently for $[Na_7(tBu_2pz)_6(OH)]$.[9] The ligands are staggered so as to be mutually perpendicular around the complex, presumably to avoid steric clashes between the bulky *tert*-butyl groups. The structure of the sodium analogue **6** is isomorphous with the lithium counterpart, with all angles similar and bond lengths longer to accommodate the larger metal ions (Table 4). The sides of the $M_8$ cube expand from 2.39 Å in the case of Li to 2.91 Å for the Na complex, as a result of the increase in ionic radius in moving from Li to Na.[12]

  

CHEMISTRY
AN ASIAN JOURNAL

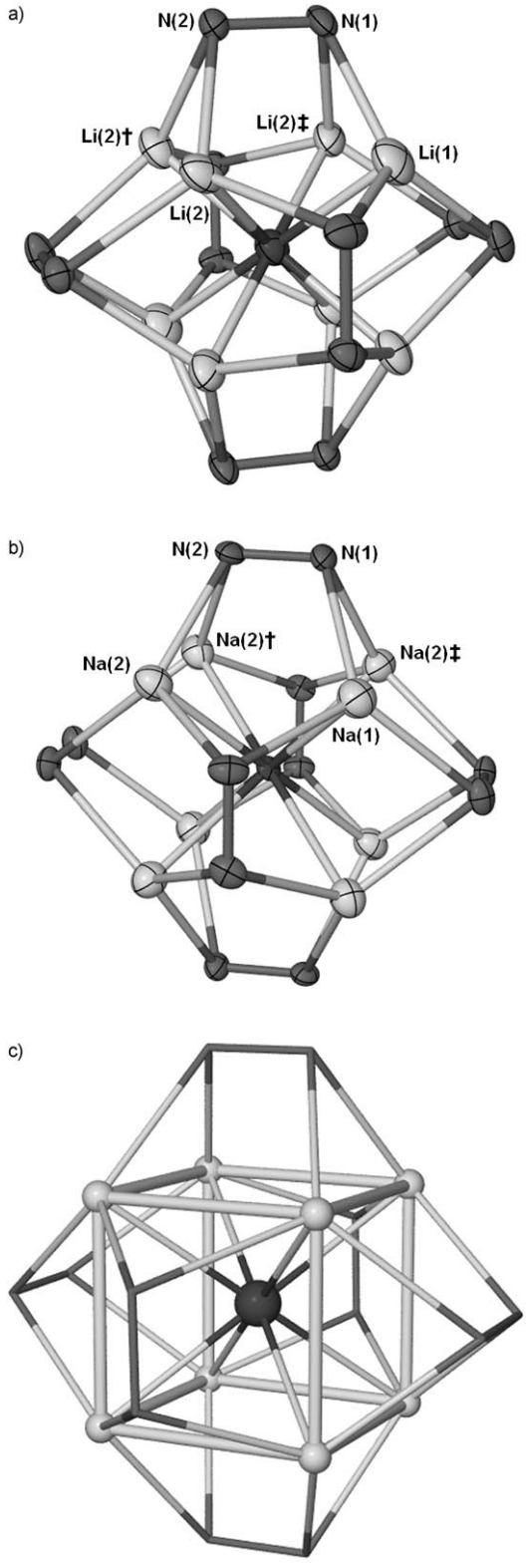


Figure 7. Central $M_8O$ units of a) $[Li_8(tBu_2pz)_6O]$ (**5**) and b) $[Na_8(tBu_2pz)_6O]$ (**6**). Only the nitrogen atoms of the pyrazolate rings are shown for clarity, ellipsoids are shown at 30% probability. Symmetry operators: † = $y, -x+y, -z$, ‡ = $-x+y, -x, z$. c) The pyrazolate ligands are situated over the faces of the $Li_8$ or $Na_8$ cube in the structures of both **5** (displayed) and **6**.

Table 4. Selected bond lengths (Å) and angles (°) for the Li and Na cage complexes **5** and **6**.[a]

| $[Li_8(tBu_2pz)_6O]$ (**5**) | | $[Na_8(tBu_2pz)_6O]$ (**6**) | |
|---|---|---|---|
| Li(1)–O(1) | 2.070(15) | Na(1)–O(1) | 2.480(5) |
| Li(2)–O(1) | 2.072(9) | Na(2)–O(1) | 2.530(3) |
| Li(1)–Li(2) | 2.394(12) | Na(1)–Na(2) | 2.910(4) |
| Li(2)–Li(2)† | 2.389(11) | Na(2)–Na(2)† | 2.905(4) |
| N(1)–Li(1) | 2.097(4) | N(1)–Na(1) | 2.426(5) |
| N(1)–Li(2)‡ | 2.100(9) | N(1)–Na(2)‡ | 2.425(5) |
| N(2)–Li(2) | 2.108(9) | N(2)–Na(2) | 2.410(5) |
| N(2)–Li(2)† | 2.097(8) | N(2)–Na(2)† | 2.413(5) |
| | | | |
| Li(1)–O(1)–Li(2) | 70.6(2) | Na(1)–O(1)–Na(2) | 71.00(6) |
| Li(2)–O(1)–Li(2)† | 70.4(2) | Na(2)–O(1)–Na(2)† | 70.06(6) |
| Li(1)–O(1)–Li(2)† | 109.4(2) | Na(1)–O(1)–Na(2)† | 109.00(6) |
| Li(2)–O(1)–Li(2)‡ | 109.6(2) | Na(2)–O(1)–Na(2)‡ | 109.94(6) |

[a] Symmetry operators as for Figure 7. Only $^1/_6$ of the molecule is described owing to symmetry.

## Conclusions

Our study of alkali-metal pyrazolates has illustrated the versatility of pyrazolate coordination. In dimeric $[Li(Ph_2pz)(OEt_2)]_2$ (**1**), the small size of the metal forces the rarely observed $\mu$-$\eta^2$:$\eta^1$ coordination mode to occur. The pseudocubane $[Na(Ph_2pz)(thf)]_4$ (**2**) has a solely $\mu_3$-$\eta^1$:$\eta^2$:$\eta^1$ pyrazolate coordination. Unsolvated $[Na(tBu_2pz)]_n$ (**3**) has two independent polymer chains that exhibit the new pyrazolate coordination modes $\mu_3$-$\eta^5$:$\eta^2$:$\eta^2$, $\mu_5$-$\eta^5$:$\eta^2$:$\eta^1$, and $\mu_3$-$\eta^4$:$\eta^2$:$\eta^1$. In the fortuitously obtained $[Na_4(tBu_2pz)_2(thf)_3(obds)]_2$ (**4**), two tetranuclear units are linked by obds bridging, and the pyrazolate groups show $\mu_3$-$\eta^1$:$\eta^2$:$\eta^1$ binding as in tetranuclear **2**. The extreme sensitivity of alkali-metal pyrazolates to hydrolysis is indicated by the isolation of crystals of the isomorphous near-cubic cages $[M_8(tBu_2pz)_6O]$ (M = Li (**5**) and Na (**6**)), in which all pyrazolates have the recently observed $\mu_4$-$\eta^1$:$\eta^1$:$\eta^1$:$\eta^1$ binding mode. In contrast with $[Na_7(tBu_2pz)_6(OH)]$,[9] which has both $\mu_4$-$\eta^1$:$\eta^1$:$\eta^1$:$\eta^1$ and $\mu_3$-$\eta^1$:$\eta^1$:$\eta^1$ coordination, **5** and **6** have exclusively the former in a highly symmetrical arrangement.

## Experimental Section

*General Remarks*

All reactions were carried out under dry nitrogen with standard Schlenk and dry-box equipment. $Et_2O$ and THF were freshly distilled over sodium/benzophenone prior to use. IR spectra (4000–650 $cm^{-1}$) were recorded as nujol mulls with a Perkin–Elmer 1600 FTIR spectrophotometer. $^1H$ and $^{13}C$ NMR spectra were recorded on a Bruker DPX 300-MHz or DRX 400-MHz spectrometer with dry (freeze-thawed over sodium metal) degassed perdeuterobenzene or perdeuterotoluene; resonances were referenced to residual hydrogen from the solvent. $^7Li$ NMR spectra were recorded on a Bruker DRX 400 and were referenced to LiCl (1 M in $D_2O$) as an external reference. Microanalysis samples were sealed in glass ampoules under purified $N_2$ and were determined by the Campbell Microanalytical Service, University of Otago, New Zealand. 3,5-Diphenylpyrazole and 3,5-di-*tert*-butylpyrazole were prepared according to the literature.[35]

  

*Syntheses*

**1**: *n*BuLi (6.34 mL of a 1.6 M solution in hexanes, 10.1 mmol) was added by a syringe to a stirring solution of $Ph_2pzH$ (1.86 g, 8.45 mmol) in $Et_2O$ (30 mL). After 1 h of stirring, the solution was concentrated to about 10 mL and cooled overnight (5 °C), which resulted in the formation of a white precipitate. The $Et_2O$ filtrate was collected by a filter cannula and concentrated to a volume of about 5 mL. Cooling of the solution to 5 °C resulted in the formation of a colorless crystalline material. IR (nujol): $\tilde{\nu}$ = 1603 (s), 1512 (w), 1289 (m), 1246 (w), 1159 (m), 1129 (m), 1068 (m), 1029 (m), 978 (m), 948 (w), 937 (w), 913 (w), 788 (w), 753 (vs), 722 (m), 689 $cm^{-1}$ (s); $^1H$ NMR (300 MHz, $C_6D_6$, 25 °C): (spectrum of precipitate showed loss of one $Et_2O$ molecule due to drying the solid under vacuum after removal of $Et_2O$ filtrate) $\delta$ = 1.06 (t, 6H, $CH_3CH_2O$ ($Et_2O$)), 3.21 (q, 4H, $CH_3CH_2O$ ($Et_2O$)), 6.73 (brs, 2H, H4 (pz)), 6.92–6.94 (brm, 10H, *m*-, *p*-H), 7.32 ppm (brs, 8H, *o*-H); variable-temperature NMR spectra ($^1H$, $^{13}C$, and $^7Li$) were obtained on the crystalline material; $^1H$ NMR (400 MHz, $C_6D_5CD_3$, 25 °C): $\delta$ = 0.87 (t, 12H, $CH_3CH_2O$ ($Et_2O$)), 3.06 (q, 8H, $CH_3CH_2O$ ($Et_2O$)), 6.78 (t, $^3J$ = 7.20 Hz, 4H, *p*-H), 6.87 (t, $^3J$ = 7.10 Hz, 8H, *m*-H), 7.14 (s, 2H, H4 (pz)), 7.18 (d, $^3J$ = 6.98 Hz, 8H, *o*-H), 7.64 ppm (brs, minor); $^1H$ NMR (400 MHz, $C_6D_5CD_3$, −40 °C): $\delta$ = 0.35 (brs, 12H, $CH_3CH_2O$ ($Et_2O$)), 0.84–0.94 (m, 3H, $Et_2O$ (minor)), 1.19–1.26 (m, 2H, $Et_2O$ (minor)), 2.66 (brs, 8H, $CH_3CH_2O$ ($Et_2O$)), 4.38 (dt, 0.40H, $Et_2O$ (minor)), 6.84–6.89 (brm, 12H, *m*-, *p*-H), 7.16 (s, 2H, H4 (pz)), 7.50 (brs, 8H, *o*-H), 7.90 ppm (d, $^2J$ = 7.39 Hz, minor); $^{13}C\{^1H\}$ NMR (100.6 MHz, $C_6D_5CD_3$, 25 °C): $\delta$ = −14.6 (s, $Et_2O$), 65.2 (s, $Et_2O$), 102.4 (s, C4 ($Ph_2pz$)), 125.3 (s, *o*-C($Ph_2pz$)), 125.8 (s, *o*-C($Ph_2pz$)), 126.4 (s, *p*-C($Ph_2pz$)), 126.7 (s, *p*-C($Ph_2pz$)), 127.2 (s, *m*-C($Ph_2pz$)), 128.8 (s, *m*-C($Ph_2pz$)), 133.4 (s, quaternary-C($Ph_2pz$)), 159.4 ppm (s, C3, C5 ($Ph_2pz$)); $^7Li$ NMR (155.5 MHz, $C_6D_6$, 25 °C): $\delta$ = −5.51 (1Li), −4.73 (0.26Li), −4.39 ppm (0.1Li); $^7Li$ NMR (155.5 MHz, $C_6D_5CD_3$, −40 °C): $\delta$ = −2.95 (1Li), −2.43 ppm (0.18Li); $^7Li$ NMR (155.5 MHz, $C_6D_5CD_3$, 40 °C): $\delta$ = −2.97 (1Li), −2.16 (0.23Li), −1.82 (0.08Li), −1.18 ppm (0.34Li); elemental analysis: calcd (%) for $C_{38}H_{42}Li_2N_4O_2$: C 75.98, H 7.05, N 9.33; found: C 74.71, 73.54, H 6.93, 6.91, N 9.87, 9.13.

**2**: $Na\{N(SiMe_3)_2\}$ (10.9 mL of a 1.0 M solution in hexanes, 10.9 mmol) was added by syringe to a stirred solution of $Ph_2pzH$ (2.41 g, 10.9 mmol) in THF (30 mL). The resulting mixture was stirred for 1 h, after which the solution was concentrated to about 10 mL. A colorless crystalline material (2.06 g, 60 %) formed upon standing at room temperature (over a few months). IR (nujol): $\tilde{\nu}$ = 1602 (s), 1511 (w), 1264 (m), 1216 (m), 1154 (w), 1068 (s), 1026 (w), 974 (s), 913 (m), 753 (vs), 722 (w), 699 (s), 689 $cm^{-1}$ (s); $^1H$ NMR (300 MHz, $C_6D_6$, 25 °C): (spectrum showed "splitting" of thf signals) $\delta$ = 1.12–1.19 (m, 16H, thf), 3.01–3.19 (m, 16H, thf), 7.05 (t, 8H, *p*-H), 7.17–7.22 (m, 20H, *m*-H, H4 (pz)), 7.85 ppm (d, 16H, *o*-H); elemental analysis: calcd (%) for $C_{76}H_{76}N_8Na_4O_4$: C 72.59, H 6.09, N 8.91; found: C 72.38, H 6.12, N 9.07.

**3**: Fortuitous synthesis: Yb metal filings (0.68 g, 3.91 mmol), $tBu_2pzH$ (0.18 g, 1.01 mmol), and Na metal (0.04 g, 1.71 mmol) were placed in a Carius tube and sealed under a vacuum of about $10^{-2}$ Torr. The Carius tube was then heated at 200 °C, and large colorless crystals formed within 30 min. The tube was left at this temperature overnight, whereby a mixture of fine yellow crystals and large colorless crystals (major product) was obtained. X-ray analysis indicated that the colorless crystals were those of **3**. Deliberate synthesis: Na metal (0.26 g, 11.5 mmol), $tBu_2pzH$ (1.31 g, 7.29 mmol), and a drop of Hg were placed in a Carius tube and sealed under a vacuum of about $10^{-2}$ Torr. The Carius tube was then heated at 200 °C, and large colorless crystals formed within 30 min. The tube was left at this temperature overnight, which resulted in a mixture of crystals and white precipitate (1.20 g, 82 %). Both crystalline material and white precipitate were identified by IR and $^1H$ NMR spectroscopy as Na($tBu_2pz$). A unit cell of the crystals confirmed the identity of the compound as **3**. IR (nujol): $\tilde{\nu}$ = 1633 (w), 1515 (m), 1498 (m), 1307 (m), 1248 (m), 1205 (w), 1016 (s), 997 (s), 880 (m), 810 (m), 779 (s), 745 (m), 726 (s), 655 $cm^{-1}$ (w); $^1H$ NMR (400 MHz, $C_6D_6$, 25 °C): $\delta$ = 1.14 (s, 54H, *t*Bu), 1.24 (s, 18H, *t*Bu) 6.10 (s, 3H, H4), 6.13 ppm (brs, 1H, H4); variable-temperature $^1H$ NMR (400 MHz, $C_7D_8$, 25 °C): $\delta$ = 1.12 (s, 54H, *t*Bu), 1.13 (s, 9H, *t*Bu), 1.25 (s, 18H, *t*Bu), 6.04 (s, 3H, H4 (pz)), 6.06 (brs, 1H, H4 (pz)), 6.07 ppm (brs, 0.5H, H4); $^1H$ NMR (400 MHz, $C_7D_8$, 60 °C): 1.10 (s, 108H, *t*Bu), 1.21 (s, 18H, *t*Bu), 6.02 (brs, 6H, H4 (pz)), 6.03 ppm (brs, 1H, H4 (pz)); $^1H$ NMR (400 MHz, $C_7D_8$, −60 °C): 1.17 (s, 162H, *t*Bu), 1.31 (s, 18H, *t*Bu), 1.33 (s, 9H, *t*Bu), 6.13 (s, 9H, H4 (pz)), 6.20 (brs, 1H, H4 (pz)), 6.25 (brs, 0.5H, H4 (pz)).

**4**: A solution of $tBu_2pzH$ (1.00 g, 5.55 mmol) in THF (75 mL) was stirred over finely chopped sodium metal (1.00 g, 43.5 mmol, washed in hexane) for 24 h in a silicone-greased Schlenk flask. The reaction mixture was left to stand for approximately six months, which resulted in the inclusion of grease from the apparatus into the solution. The solution of THF was removed by a filter cannula and concentrated to about 20 mL. Crystals formed after approximately one week at 3 °C and were identified by X-ray crystallography as $[Na_4(tBu_2pz)_2(thf)_3(obds)]_2$. IR (nujol): $\tilde{\nu}$ = 3105 (m), 1615 (w), 1508 (m), 1492 (m), 1398 (m), 1310 (vs), 1247 (vs), 1204 (m), 1073 (s), 1014 (m), 998 (s), 953 (m), 914 (ms), 837 (m), 804 (w), 767 (vs), 680 (w), 638 $cm^{-1}$ (w); $^1H$ NMR (300 MHz, $C_6D_6$, 25 °C): $\delta$ = 1.14 (s, 72H, *t*Bu), 1.26 (s, 24H, obds), 1.39–1.45 (m, 24H, thf), 3.52–3.57 (m, 24H, thf), 6.09 ppm (s, 4H, H4 (pz)); $^{13}C\{^1H\}$ NMR (100.6 MHz, $C_6D_6$, 25 °C): $\delta$ = 25.8 (s, $CH_2$ (thf)), 31.6 (s, *t*Bu), 32.0 (s, $Me_2Si$) 67.8 (s, $CH_2O$ (thf)), 96.9 (C4), 165.5 ppm (C3, C5). After removal of THF under reduced pressure a white precipitate was obtained, which was identified by $^1H$ NMR spectroscopy as mainly $[Na(tBu_2pz)(thf)]_n$ (1.47 g, ≈70 %). IR (nujol): $\tilde{\nu}$ = 3106 (w), 1618 (m), 1510 (m), 1496 (m), 1398 (m), 1359 (s), 1306 (s), 1248 (vs), 1206 (s), 1053 (vs), 1014 (vs), 997 (s), 954 (w), 916 (m), 895 (m), 836 (w), 798 (m), 773 (vs), 724 (vs), 628 $cm^{-1}$ (m); $^1H$ NMR (300 MHz, $C_6D_6$, 25 °C): (spectrum of white precipitate showed two different pyrazolate environments, presumably attributable to [Na($tBu_2pz$)(thf)] and an unsolvated [Na($tBu_2pz$)] species in a 3:1 ratio) $\delta$ = 1.14 (s, 18H, *t*Bu), 1.31 (s, 54H, *t*Bu), 1.37–1.41 (brm, 12H, thf), 3.38–3.51 (brm, 12H, thf), 6.09 (brs, 3H, H4 (pz)), 6.10 ppm (brs, 1H, H4 (pz)); elemental analysis: calcd (%) for $C_{15}H_{27}N_2NaO$: C 65.66, H 9.91, N 10.21; found: C 62.53, H 9.66, N 10.42.

**5**: *n*BuLi (7.71 mL of a 1.6 M solution in hexanes, 12.3 mmol) was added dropwise to a solution of $tBu_2pzH$ (1.85 g, 10.3 mmol) in $Et_2O$ (50 mL). The resulting solution was stirred for 1 h, after which it was concentrated to about 25 mL. Cooling of the solution to 5 °C resulted in a small amount of colorless crystalline material. IR (nujol): $\tilde{\nu}$ = 1568 (w), 1504 (m), 1404 (w), 1306 (s), 1250 (s), 1213 (m), 1125 (m), 1028 (s), 1002 (s), 940 (w), 794 (s), 734 (s), 632 (m), 501 $cm^{-1}$ (w); $^1H$ NMR (300 MHz, $C_6D_6$, 25 °C): $\delta$ = 1.21 (s, 108H, *t*Bu), 6.01 ppm (s, 6H, H4 (pz)).

**6**: $tBu_2pzH$ (0.50 g, 2.77 mmol) was dissolved in toluene (50 mL) and stirred over finely chopped sodium metal (0.50 g, 21.75 mmol, washed in hexane) for 24 h at room temperature. The solution was recovered by filtration, concentrated, and left to stand at room temperature for one week, during which a small amount of colorless crystalline product formed. $^1H$ NMR (300 MHz, $C_6D_6$, 25 °C): $\delta$ = 1.14 (s, 108H, *t*Bu), 6.09 ppm (s, 6H, H4 (pz)).

*Crystallographic Data and Refinement*

Complexes **1**–**4** and the cage complexes **5** and **6** were mounted on glass fibers in viscous hydrocarbon oil. Crystal data were collected with a Nonius Kappa CCD instrument with monochromated $Mo_{K\alpha}$ radiation ($\lambda$ = 0.71073 Å). All data were collected at 123 K maintained by an open flow of nitrogen in an Oxford Cryostreams cryostat. X-ray data were processed with the DENZO program.[36] Structures were solved by direct methods with SHELXS-97[37] and refined by full-matrix least squares against $F^2$ of all reflections with SHELXL-97[38] and the graphical interface X-Seed.[39] Non-hydrogen atoms were refined anisotropically. All hydrogen atoms were placed in calculated positions with the riding model.

The structure of **3** contains one disordered *tert*-butyl group, which was successfully modeled over two positions. The structure of **4** contains two disordered *tert*-butyl groups, the occupancies of which were allowed to refine freely. One *t*Bu group required AFIX and SADI restraints to be applied.

The structures of both **5** and **6** contain significant disorder of the *t*Bu groups, as evidenced by large thermal ellipsoids. The high symmetry of the structure is clearly a description of the central core unit and not an accurate reflection of the pendant groups. The Na structure **6** contains

  

what appears to be disordered hexane over a special position which was refined isotropically with no hydrogen atoms added. The Li structure **5** contains some residual electron density in a similar position, although any solvent here appeared highly disordered and with partial occupancy and therefore cannot be accurately included in the final model. In both cases, solvent was not observed in the $^1$H NMR spectra as the samples were dried prior to analysis, and the crystals showed signs of rapid solvent loss under a microscope.

CCDC-612579 (**1**), -612580 (**2**), -632619 (**3**), -612581 (**4**), -612582 (**5**), and -612583 (**6**) contain the supplementary crystallographic data (excluding structure factors) for this paper. These data can be obtained free of charge from the Cambridge Crystallographic Data Centre, 12 Union Road, Cambridge, CB2 1EZ, UK (fax: (+44) 1223-336-033; e-mail: deposit@ccdc.cam.ac.uk) or at www.ccdc.cam.ac.uk/data_request.cif.

**1**: $C_{38}H_{42}Li_2N_4O_2$, $M_r = 600.64$, colorless block, $0.35 \times 0.32 \times 0.30$ mm$^3$, triclinic, space group $P\bar{1}$ (No. 2), $a = 8.0614(2)$, $b = 9.8482(3)$, $c = 11.7819(5)$ Å, $\alpha = 107.699(1)$, $\beta = 98.410(1)$, $\gamma = 101.873(1)°$, $V = 849.88(5)$ Å$^3$, $Z = 1$, $\rho_{cald} = 1.174$ g cm$^{-3}$, $F_{000} = 320$, $2\theta_{max} = 55.0°$, 14585 reflections collected, 3895 unique ($R_{int} = 0.0792$). Final GoF = 0.995, $R1 = 0.0504$, $wR2 = 0.1072$, $R$ indices based on 2351 reflections with $I > 2\sigma(I)$ (refinement on $F^2$), 210 parameters, no restraints. Lp and absorption corrections applied, $\mu = 0.072$ mm$^{-1}$.

**2**: $C_{76}H_{76}N_8Na_4O_4$, $M_r = 1257.41$, colorless needle, $0.40 \times 0.20 \times 0.05$ mm$^3$, monoclinic, space group $C2/c$ (No. 15), $a = 25.550(5)$, $b = 12.490(3)$, $c = 24.420(5)$ Å, $\beta = 118.54(3)°$, $V = 6846(2)$ Å$^3$, $Z = 4$, $\rho_{cald} = 1.220$ g cm$^{-3}$, $F_{000} = 2656$, $2\theta_{max} = 55.0°$, 31229 reflections collected, 7808 unique ($R_{int} = 0.1024$). Final GoF = 1.017, $R1 = 0.0670$, $wR2 = 0.1133$, $R$ indices based on 3667 reflections with $I > 2\sigma(I)$ (refinement on $F^2$), 415 parameters, no restraints. Lp and absorption corrections applied, $\mu = 0.098$ mm$^{-1}$.

**3**: $C_{99}H_{171}N_{18}Na_9$, $M_r = 1820.45$, colorless rod, $0.25 \times 0.18 \times 0.17$ mm$^3$, triclinic, space group $P\bar{1}$ (No. 2), $a = 15.0632(5)$, $b = 19.9474(8)$, $c = 20.1230(5)$ Å, $\alpha = 69.2910(10)$, $\beta = 75.6470(10)$, $\gamma = 83.697(3)°$, $V = 5477.6(3)$ Å$^3$, $Z = 2$, $\rho_{cald} = 1.104$ g cm$^{-3}$, $F_{000} = 1980$, $2\theta_{max} = 50.0°$, 46604 reflections collected, 19230 unique ($R_{int} = 0.0970$). Final GoF = 1.014, $R1 = 0.0766$, $wR2 = 0.1483$, $R$ indices based on 8552 reflections with $I > 2\sigma(I)$ (refinement on $F^2$), 1220 parameters, 12 restraints. Lp and absorption corrections applied, $\mu = 0.096$ mm$^{-1}$.

**4**: $C_{76}H_{148}N_8Na_8O_{12}Si_4$, $M_r = 1662.30$, colorless block, $0.18 \times 0.16 \times 0.12$ mm$^3$, monoclinic, space group $P2_1/c$ (No. 14), $a = 12.858(3)$, $b = 21.160(4)$, $c = 18.693(4)$ Å, $\beta = 105.33(3)°$, $V = 4905.2(17)$ Å$^3$, $Z = 2$, $\rho_{cald} = 1.125$ g cm$^{-3}$, $F_{000} = 1800$, $2\theta_{max} = 52.0°$, 31035 reflections collected, 9624 unique ($R_{int} = 0.1163$). Final GoF = 1.016, $R1 = 0.0728$, $wR2 = 0.1322$, $R$ indices based on 4818 reflections with $I > 2\sigma(I)$ (refinement on $F^2$), 565 parameters, nine restraints. Lp and absorption corrections applied, $\mu = 0.150$ mm$^{-1}$.

**5**: $C_{66}H_{114}Li_8N_{12}O$, $M_r = 1147.21$, colorless plate, $0.14 \times 0.12 \times 0.08$ mm$^3$, trigonal, space group $R\bar{3}$ (No. 148), $a = b = 14.1079(3)$, $c = 33.8466(4)$ Å, $V = 5834.05(19)$ Å$^3$, $Z = 3$, $\rho_{cald} = 0.980$ g cm$^{-3}$, $F_{000} = 1878$, $2\theta_{max} = 50.0°$, 23090 reflections collected, 2284 unique ($R_{int} = 0.1012$). Final GoF = 1.249, $R1 = 0.1442$, $wR2 = 0.3210$, $R$ indices based on 1862 reflections with $I > 2\sigma(I)$ (refinement on $F^2$), 208 parameters, no restraints. Lp and absorption corrections applied, $\mu = 0.057$ mm$^{-1}$.

**6**: $C_{72}H_{128}N_{12}Na_8O$, $M_r = 1361.78$, colorless plate, $0.12 \times 0.12 \times 0.06$ mm$^3$, trigonal, space group $R\bar{3}$ (No. 148), $a = b = 14.399(2)$, $c = 34.744(7)$ Å, $V = 6238.4(17)$ Å$^3$, $Z = 3$, $\rho_{cald} = 1.087$ g cm$^{-3}$, $F_{000} = 2220$, $2\theta_{max} = 50.0°$, 14938 reflections collected, 2429 unique ($R_{int} = 0.1105$). Final GoF = 1.116, $R1 = 0.1414$, $wR2 = 0.3058$, $R$ indices based on 1522 reflections with $I > 2\sigma(I)$ (refinement on $F^2$), 180 parameters, no restraints. Lp and absorption corrections applied, $\mu = 0.101$ mm$^{-1}$.

## Acknowledgements

The authors gratefully acknowledge the financial support of the Australian Research Council.

[1] a) S. Trofimenko, *Chem. Rev.* **1972**, *72*, 497–509; b) S. Trofimenko, *Prog. Inorg. Chem.* **1986**, *34*, 115–210; c) G. La Monica, G. Ardizzoia, *Prog. Inorg. Chem.* **1997**, *46*, 151–238; d) A. P. Sadimenko, S. S. Basson, *Coord. Chem. Rev.* **1996**, *147*, 247–297; e) J. E. Cosgriff, G. B. Deacon, *Angew. Chem.* **1998**, *110*, 298–299; *Angew. Chem. Int. Ed.* **1998**, *37*, 286–287; f) F. Nief, *Eur. J. Inorg. Chem.* **2001**, 891–904; g) A. P. Sadimenko, *Adv. Heterocycl. Chem.* **2001**, *80*, 157–252.

[2] a) J. R. Perera, M. J. Heeg, H. B. Schlegel, C. H. Winter, *J. Am. Chem. Soc.* **1999**, *121*, 4536–4537; b) G. B. Deacon, C. M. Forsyth, A. Gitlits, B. W. Skelton, A. H. White, *Dalton Trans.* **2004**, 1239–1247; c) G. B. Deacon, A. Gitlits, P. Roesky, M. R. Burgstein, K. C. Lim, B. W. Skelton, A. H. White, *Chem. Eur. J.* **2001**, *7*, 127–138; d) G. B. Deacon, E. E. Delbridge, C. M. Forsyth, *Angew. Chem.* **1999**, *111*, 1880–1882; *Angew. Chem. Int. Ed.* **1999**, *38*, 1766–1767; e) G. B. Deacon, A. Gitlits, B. W. Skelton, A. H. White, *Chem. Commun.* **1999**, 1213–1214; f) G. B. Deacon, E. E. Delbridge, B. W. Skelton, A. H. White, *Angew. Chem.* **1998**, *110*, 2372–2373; *Angew. Chem. Int. Ed.* **1998**, *37*, 2251–2252; g) G. B. Deacon, C. M. Forsyth, A. Gitlits, R. Harika, P. C. Junk, B. W. Skelton, A. H. White, *Angew. Chem.* **2002**, *114*, 3383–3385; *Angew. Chem. Int. Ed.* **2002**, *41*, 3249–3251; h) G. B. Deacon, E. E. Delbridge, D. J. Evans, R. Harika, P. C. Junk, B. W. Skelton, A. H. White, *Chem. Eur. J.* **2004**, *10*, 1193–1204; i) G. B. Deacon, E. E. Delbridge, C. M. Forsyth, B. W. Skelton, A. H. White, *J. Chem. Soc. Dalton Trans.* **2000**, 745–751; j) C. Yélamos, M. J. Heeg, C. H. Winter, *Inorg. Chem.* **1998**, *37*, 3892–3894; k) L. R. Falvello, J. Forniés, A. Martín, V. Sicilia, P. Villarroya, *Chem. Commun.* **1998**, 2429–2430.

[3] a) I. A. Guzei, A. G. Baboul, G. P. A. Yap, A. L. Rheingold, H. B. Schlegel, C. H. Winter, *J. Am. Chem. Soc.* **1997**, *119*, 3387–3388; b) I. A. Guzei, G. P. A. Yap, C. H. Winter, *Inorg. Chem.* **1997**, *36*, 1738–1739; c) C. Yélamos, M. J. Heeg, C. H. Winter, *Inorg. Chem.* **1999**, *38*, 1871–1878; d) N. C. Mösch-Zanetti, R. Kratzner, C. Lehmann, T. R. Schneider, I. Uson, *Eur. J. Inorg. Chem.* **2000**, 13–16.

[4] a) G. B. Deacon, E. E. Delbridge, C. M. Forsyth, P. C. Junk, B. W. Skelton, A. H. White, *Aust. J. Chem.* **1999**, *52*, 733–739; b) K. R. Gust, J. E. Knox, M. J. Heeg, H. B. Schlegel, C. H. Winter, *Angew. Chem.* **2002**, *114*, 1661–1664; *Angew. Chem. Int. Ed.* **2002**, *41*, 1591–1594; K. R. Gust, J. E. Knox, M. J. Heeg, H. B. Schlegel, C. H. Winter, *Angew. Chem.* **2002**, *114*, 1661–1664; c) D. Pfeiffer, M. J. Heeg, C. H. Winter, *Angew. Chem.* **1998**, *110*, 2674–76; *Angew. Chem. Int. Ed.* **1998**, *37*, 2517–2519; D. Pfeiffer, M. J. Heeg, C. H. Winter, *Angew. Chem.* **1998**, *110*, 2674–2676; d) D. Pfeiffer, M. J. Heeg, C. H. Winter, *Inorg. Chem.* **2000**, *39*, 2377–2384.

[5] a) J. Hitzbleck, G. B. Deacon, K. Ruhlandt-Senge, *Angew. Chem.* **2004**, *116*, 5330–5332; *Angew. Chem. Int. Ed.* **2004**, *43*, 5218–5220; b) J. Hitzbleck, A. Y. O'Brien, C. M. Forsyth, G. B. Deacon, K. Ruhlandt-Senge, *Chem. Eur. J.* **2004**, *10*, 3315–3323; c) J. Hitzbleck, A. Y. O'Brien, G. B. Deacon, K. Ruhlandt-Senge, *Inorg. Chem.* **2006**, *45*, 10329–10337; d) K. Most, S. Köpke, F. Dall'Antonia, N. C. Mösch-Zanetti, *Chem. Commun.* **2002**, 1676–1677; e) K. Most, N. C. Mösch-Zanetti, D. Vidovic, J. Magull, *Organometallics* **2003**, *22*, 5485–5490.

[6] S. Trofimenko, *Scorpionates: The Coordination Chemistry of Poly-(pyrazolyl)borate Ligands*, Imperial College Press, London, **1999**.

[7] W. Zheng, M. J. Heeg, C. H. Winter, *Eur. J. Inorg. Chem.* **2004**, 2652–2657.

[8] T. Beringhelli, G. D'Alfonso, M. Panigati, P. Mercandelli, A. Sironi, *Chem. Eur. J.* **2002**, *8*, 5340–5350.

[9] S.-A. Cortés-Llamas, R. Hernández-Lamoneda, M.-A. Velázquez-Carmona, M.-A. Muñoz-Hernández, R. A. Toscano, *Inorg. Chem.* **2006**, *45*, 286–294.

[10] G. Meyer, *J. Alloys Compd.* **2000**, *300–301*, 113–122.

[11] a) M. L. Cole, P. C. Junk, L. M. Louis, *J. Chem. Soc. Dalton Trans.* **2002**, 3906–3914; b) M. L. Cole, A. J. Davies, C. Jones, P. C. Junk, *J. Organomet. Chem.* **2004**, *689*, 3093–3107; c) J. Baldamus, C. Berghof, M. L Cole, E. Hey-Hawkins, P. C. Junk, L. M. Louis, *Eur. J. Inorg. Chem.* **2002**, 2878–2884; d) M. L. Cole, P. C. Junk, *Chem. Commun.* **2007**, DOI: 10.1039/b613984.

[12] R. D. Shannon, *Acta Crystallog. Sect. A* **1976**, *32*, 751–767.

  

[13] a) W. Zheng, M. J. Heeg, C. H. Winter, *Angew. Chem. Int. Ed.* **2003**, *42*, 2761–2764; *Angew. Chem.* **2003**, *115*, 2867–2870; b) H. Nöth, H. Sachdev, M. Schmidt, H. Schwenk, *Chem. Ber.* **1995**, *128*, 105–113.
[14] F. A. Cotton, S. C. Haefner, J. H. Matonic, X. Wang, C. A. Murillo, *Polyhedron* **1997**, *16*, 541–550.
[15] N. G. Connelly, P. M. Hopkins, A. G. Orpen, G. M. Rosair, F. Viguri, *J. Chem. Soc. Dalton Trans.* **1992**, 2907–2908.
[16] M. F. Lappert, M. J. Slade, A. Singh, J. L. Atwood, R. D. Rogers, R. Shakir, *J. Am. Chem. Soc.* **1983**, *105*, 302–304.
[17] M. G. Gardiner, C. L. Raston, *Inorg. Chem.* **1996**, *35*, 4162–4169.
[18] J. T. B. H. Jastrzebski, G. van Koten, K. Goubitz, C. Arlen, M. Pfeffer, *J. Organomet. Chem.* **1983**, *246*, C75-C79.
[19] D. Rutherford, D. A. Atwood, *J. Am. Chem. Soc.* **1996**, *118*, 11535–11540.
[20] W. J. Evans, *Polyhedron* **1987**, *6*, 803–835.
[21] T. J. Boyle, D. M. Pedrotty, T. M. Alam, S. C. Vick, M. A. Rodriguez, *Inorg. Chem.* **2000**, *39*, 5133–5146.
[22] T. J. Boyle, N. L. Andrews, M. A. Rodriguez, C. Campana, T. Yiu, *Inorg. Chem.* **2003**, *42*, 5357–5366.
[23] J. Geier, H. Ruegger, H. Grutzmacher, *Dalton Trans.* **2006**, 129–136.
[24] J.-F. Le Maréchal, C. Villiers, P. Charpin, M. Lance, M. Nierlich, J. Vigner, M. Ephritikhine, *J. Chem. Soc. Chem. Commun.* **1989**, 308–310.
[25] W. J. Evans, M. S. Sollberger, J. L. Shreeve, J. M. Olofson, J. H. Hain, Jr., J. W. Ziller, *Inorg. Chem.* **1992**, *31*, 2492–2501.
[26] M. L. Cole, C. Jones, P. C. Junk, *J. Chem. Soc. Dalton Trans.* **2002**, 896–905.
[27] T. Aoyagi, H. M. M. Shearer, K. Wade, G. Whitehead, *J. Organomet. Chem.* **1979**, *175*, 21–32.
[28] K. W. Klinkhammer, *Chem. Eur. J.* **1997**, *3*, 1418–1431.
[29] R. Wochele, W. Scwarz, K. W. Klinkhammer, K. Locke, J. Weidlein, *Z. Anorg. Allg. Chem.* **2000**, *626*, 1963–1973.
[30] S. Chadwick, U. Englich, K. Ruhlandt-Senge, *Organometallics* **1997**, *16*, 5792–5803.
[31] L. Rösch, G. Altnan, C. Krüger, Y.-H. Tsay, *Z. Naturforsch.* **1983**, *38b*, 34–41.
[32] a) I. Haiduc, *Organometallics* **2004**, *23*, 3–8; b) V. Lorenz, A. Fischer, S. Gießmann, J. W. Gilje, Y. Gun'ko, K. Jacob, F. T. Edelmann, *Coord. Chem. Rev.* **2000**, *206–207*, 321–368; c) F. T. Edelmann, S. Gießmann, A. Fischer, *J. Organomet. Chem.* **2001**, *620*, 80–89; d) M. Cazacu, A. Vlad, M. Marcu, C. Racles, A. Airinei, G. Munteanu, *Macromolecules* **2006**, *39*, 3786–3793; e) F. T. Edelmann, S. Gießmann, A. Fischer, *Chem. Commun.* **2000**, 2153–2154; f) V. Lorenz, A. Fischer, F. T. Edelmann, *Inorg. Chem. Commun.* **2000**, *3*, 292–295; g) F. T. Edelmann, S. Gießmann, A. Fischer, *Inorg. Chem. Commun.* **2000**, *3*, 658–661.
[33] a) S. Harvey, M. F. Lappert, C. L. Raston, B. W. Skelton, G. Srivastava, A. H. White, *J. Chem. Soc. Chem. Commun.* **1988**, 1216–1217; b) A. Steiner, G.T Lawson, B. Walfort, D. Leusser, D. Stalke, *J. Chem. Soc. Dalton Trans.* **2001**, 219–221.
[34] A. Bondi, *J. Phys. Chem.* **1964**, *68*, 441–451.
[35] J. Elguero, E. Gonzalez, R. Jacquier, *Bull. Soc. Chim. Fr.* **1968**, 707–713.
[36] Z. Otwinowski, W. Minor in *Macromolecular Crystallography*, *Part A*, *Methods in Enzymology*, *Vol. 276*, (Eds.: C. Carter, Jr., R. Sweet, J. Abelson, M. Simon), Academic Press, New York, **1997**.
[37] G. M. Sheldrick, SHELXS-97, University of Göttingen, Göttingen (Germany), **1997**.
[38] G. M. Sheldrick, SHELXL-97, University of Göttingen, Göttingen (Germany), **1997**.
[39] L. J. Barbour, *J. Supramol. Chem.* **2003**, *1*, 189–191.

Received: January 9, 2007

  